Кінетична турбіна з чашоподібними лопатями має низьку продуктивність. Це недорога, проста у виготовленні і встановленні турбіна. Кінетичні турбіни виробляються спеціально для сільської місцевості, яка може знаходитися далеко від технологічних об'єктів. Причина, з якої дані турбіни все ще використовуються, полягає в забезпеченні електроенергією сільських районів. Дослідження такої кінетичної турбіни з чашоподібними лопатями все ще проводяться, хоча і не так часто. Багато зусиль було докладено для поліпшення кінетичних характеристик турбіни. Дане імітаційне дослідження було проведено для порівняння звичайної кінетичної турбіни з чашоподібними лопатями з кінетичною турбіною з додатковою рульовою лопаттю на предмет підвищення продуктивності турбіни.

Про продуктивність кінетичної турбіни можна судити за величиною тиску або імпульсу, що виникає між двома лопатями.

Метою проведеного моделювання є перевірка тиску, який виникає в чотирьох послідовних лопатях, які контактують з початковим потоком води. Перевірка цього тиску виконується при кожному 5-градусному переміщенні колеса турбіни, починаючи з a=45° до a=45°, таким чином буде отримано дев'ять пар результатів порівняння продуктивності кінетичної турбіни з чашоподібними лопатями.

На звичайній кінетичній турбіні з чашоподібними лопатями можна побачити, що потік води, що надходить в область турбіни, після підштовхування першої лопаті прямує в зону виходу турбіни. Таким чином, вважається, що має місце потенційна втрата енергії води.

Моделювання кінетичної турбіни з чашоподібними лопатями з рульовою лопаттю показує, що тиск на лопаті збільшується. Потік води, що покинув область турбіни, може чинити додатковий тиск на решту лопатки турбіни. При побудові графіка значення тиску результату моделювання стає ясно, що після приєднання рульової лопаті спостерігається підвищення продуктивності турбіни

Ключові слова: чашоподібна лопать, кінетична турбіна, сільська місцевість, рульова лопать, імпульс, продуктивність

UDC 621.31
DOI: 10.15587/1729-4061.2019.173986

BOWL BLADED HYDROKINETIC TURBINE WITH ADDITIONAL STEERING BLADE NUMERICAL MODELING

Rudy Soenoko
Doctor of Technological Sciences, Professor*
E-mail: rudysoen@ub.ac.id
Purnami
Doctorate*
E-mail: purnami.ftub@ub.ac.id
*Department of Mechanical Engineering
Brawijaya University
Jalan. Mayjend Haryono, 167,
Malang, Indonesia, 65145

Received date 28.03.2019
Accepted date 13.07.2019
Published date 19.08.2019

1. Introduction

Kinetic turbine is a turbine that relies on water flow rate or kinetic energy. There are two types of kinetic turbines that have been studied, namely the curve bladed kinetic turbine and the bowl bladed kinetic turbine (BBKT). Both types of turbines are developed because they are easy to manufacture and easy to maintain and are often found in rural areas [1, 2]. Because of its simplicity, this turbine has a low efficiency.

Discussing hydrokinetic turbines is interesting, because this type of turbine is a simple turbine that utilizes kinetic energy. This turbine is not costly, easy to make, easy to install, easy to operate and easy to maintain. The main problem is the low turbine performance. The hydrokinetic turbine is the development of a horizontal axis water wheel. A hydrokinetic turbine technology was adopted from a horizontal axis water wheel.

Although there have been many kinetic turbine problems that have been solved in the field based on the water flow behavior, but there are still no studies solving the problem officially published internationally. Most scientists are aware of the low kinetic turbine performance. Many factors are suspected to be the cause of this low performance, one of which is the behavior of water entering the turbine room area.

Although this turbine is simple, it does not mean that this turbine does not need to be improved. An innovative investigation is needed to improve this kinetic turbine. Because the slightest increase in performance is very meaningful for a small scale water power plant.

Therefore, it is necessary to conduct a special study that utilizes basic knowledge about water flow behavior. Especially the water flow behavior that discusses the thrust generated on the turbine blade. In this case, the basis used is the momentum for each turbine blade. Increasing the amount of water that drives the blade can ensure that the momentum will be even greater. So it was decided to examine this turbine kinetic by adding a steering blade. The purpose of the addition of the steering blade is for more blades to gain momentum of the water.

2. Literature review and problem statement

Turbine kinetic simulation studies for tidal currents have also been carried out to obtain the optimal turbine performance [3, 4]. While the steering blade addition was adopted from the study entitled Investigation on the Performance of a Modified Savonius Water Turbine with Single and Two

Deflector Plates [5]. Another research was about the variable openings that regulate a steering blade that will determine the work of the cross flow turbine [6, 7].

Research on kinetic performance of standard turbines, published in international journals, is very little. There are many studies on this turbine kinetic test, but none are published internationally. Most of these turbine kinetic test studies are published in national level journals.

A study about an approach for hydrokinetic dynamic behavior [8] mentioned that the study was conducted to find out how to improve the hydrokinetic turbine performance. In this study, it was stated that it is necessary to develop capable methods of implementing efficient hydroelectric systems. Mechanical losses are the focus of this study, so that this study is focusing on shaft coupling by implementing a speed multiplier. Another study [9] introduces a magnetic coupling to improve the turbine efficiency. This study attempts to solve the low turbine efficiency by minimizing the mechanical loss.

Other studies discuss the kinetic turbine by varying the blade numbers and the directional plate angle variations [10]. Which actually indicates a problem with water flow behavior in the turbine.

Similarly, the study suggested the Darrieus hydrokinetic turbine [11]. Where the kinetic turbine adopted from the wind turbine is believed to provide a better hydrokinetic turbine performance.

A cascade turbine called Vertical Axis Hydrokinetic Turbine – Straight-Blade Cascaded (VAHT-SBC) was discussed with three variations in the blade number that compare the experimental and numerical simulation result tests [12]. The purpose of this study is to review, which VAHT-SBC model has the best performance.

A study conducted a CFD analysis to compare several variations of three turbine positions to obtain a best turbine position to produce the best turbine performance [13]. At a glance, it appears that this study actually discusses the water flow behavior that occurs in the turbine area.

This article discusses computer code algorithms to calculate the performance characteristics of ducted axial-flow hydrokinetic turbines [14]. One of the goals is to detect vortex and cavitation. It is seen that the water flow behavior in the turbine is observed in this study.

Other paper reviews work involving small axial flow hydrokinetic turbines specifically for generating electricity for remote communities outside the network and suggests improvements to overcome major problems. However, some deployments have experienced major problems with debris attached to the turbines, which resulted in disrupted operations. Again, this is related to the flow of water entering the turbine [15].

A study of hydrokinetic which has a hinge that moves the blade towards the outer side when it gets a water pressure on the blade back side. The purpose of the blade construction of the kinetic turbine is to reduce the negative forces occurrence. Where this negative force will produce a negative momentum, which finally would lower the turbine performance [16].

From several studies that have been mentioned, the objective of these studies is to obtain better performance of the hydrokinetic turbine. All topics discuss design optimization, which actually talks about the water flow. One thing that has not been observed in depth is how water flow behaves in the turbine area. How does the water flow push the blades. Does the water flow speed really produce a force on the blades, which is strongly related to the turbine performance. A study about a Bowl Bladed Hydro Kinetic Turbine Performance [17] shows that the water flow just pushes one blade. From all the reviews above, it is very necessary to conduct a CFD study on bowl bladed kinetic turbine with an additional steering blade. With this numerical modeling, water flow behavior will be seen. Hopefully, this bowl bladed kinetic turbine with a steering blade will improve the performance of hydrokinetic.

3. The aim and objectives of the study

The aim of the study is to investigate the bowl bladed kinetic turbine performance with a steering blade, using a Computer Fluid Dynamic Simulation.

To achieve this aim, the following objectives are accomplished:

– does the turbine performance increase after attaching with a steering blade;

– is there an increase in momentum with an additional steering blade, for each area between 2 blades;

– is there an increase in momentum in areas covering 4 blades reviewed;

– how many blades get a large water pressure.

4. Basic definitions

4. 1. Kinetic turbine

As explained above, the kinetic turbine is a simple turbine that can produce electrical energy, but its performance is low, the electricity quality is low, because the rotation is not stable and can only produce low-quality electricity. Curve bladed kinetic turbine has been studied in the laboratory. The research conducted was to test the turbine model on a laboratory scale [10, 11]. The laboratory scale kinetic turbine test results show a low turbine performance. The results of this low laboratory test triggered the researchers to find out the cause. One of the allegations of this low efficiency is that the blade is not maximally pushed. Research then continued by conducting a simulation test with the computational fluid dynamic software. The objective of using this CFD software is to find out the water flow behavior and observe the amount of pressure on the turbine blade. The pressure on the turbine blade will generate momentum and eventually be converted into a turbine torque. This curve blade kinetic turbine simulation research adjusts to the dimensions and test conditions that are the same as the size and conditions of the tests carried out in the laboratory [18]. From the test results, it was found that the water flow that drives the turbine blade only produces a small momentum. The reason is that only a few blades are driven by the water flow, because the water flow, after pushing one blade, was directly going out into the turbine output. This is what is suspected to be the cause of the low turbine performance. Because water flow that still has kinetic energy leaves the turbine area immediately. From the results of this evaluation, CFD simulation studies were continued by adding a steering blade on the turbine [3]. The purpose of installing this blade is expected to be able to hold the water out directly into the turbine outlet, so that this water flow can increase the impulse on the next blade. From the simulation results, it was found that the pressure between the

two blades increased, which meant that turbine momentum increased and finally would increase the turbine torque. The turbine torque increase would surely increase the turbine efficiency. By applying or assuming a certain turbine rotation, from the simulation results, the turbine power and turbine efficiency values will be obtained. In fact, in the study of the bladed kinetic turbine conducted [12], it was seen that the bowl bladed kinetic turbine had a better performance than the curved blade kinetic turbine. However, because both types of kinetic turbines have been present in several places, the research of these two types of kinetic turbines has always been developed. Because it was felt that the bowl bladed kinetic turbine was considered to still have a low performance, further research was carried out by conducting this study of bowl bladed kinetic turbine simulation [19]. From the results of the simulation research with this bowl bladed kinetic turbine CFD, it was also concluded that there was a water flow that immediately left the turbine area after pushing just one blade. The simulation results show that the bowl bladed kinetic turbine has a better performance compared to the performance of the curve bladed kinetic turbine. While the curved bladed kinetic turbine with a steering blade has a better performance than the bowl bladed kinetic turbine. The low bowl bladed kinetic turbine performance has probably the same problem occurred on the curve bladed kinetic turbine, which is the presence of water flow that immediately leaves the turbine area after pushing just one blade. An illustration of this phenomenon can be seen from the simulation results in Fig. 1.

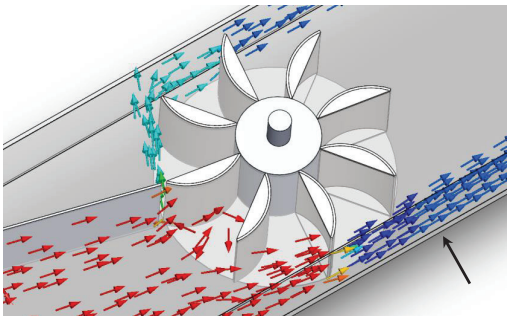

Fig. 1. Water flow leaving the turbine area

In this study, the activity was to simulate a bowl bladed kinetic turbine with an additional steering blade. The aim is to do a simulation evaluation as has been done on the curve bladed kinetic turbine. It is expected that the overall kinetic momentum of this turbine will increase. The turbine blade gets a larger boost, because the water flow was directed to pound the blade as much as possible.

The momentum theory states that the increase in pressure on the blade will increase the momentum.

4. 2. Momentum

Jet impact is based on a collision event, in this case the collision between a fluid jet flow and a blade. This underlying theory is the theory of momentum for fluid (Fig. 2).

General form of fluid momentum theory: Impulse = = Momentum change [15]:

$$F\cdot t = m\cdot\left(V_1 - V_2\right),$$

$$F = \frac{m}{t}\cdot\left(V_1 - V_2\right).$$

Fluid Mass Flow:

$$m = \rho\cdot V = \rho\cdot A\cdot X,$$

$$F = \rho\cdot A\cdot\frac{X}{t}\left(V_1 - V_2\right),$$

where ρ – density, kg/m^3; A – Jet cross-sectional area, m^2; V – Fluid Velocity, m/s; F – Force acting on the blade, N; X – Fluid Length; $X/t = V$ = speed.

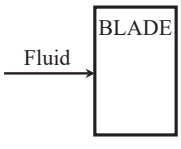

Fig. 2. Momentum

4. 3. Flat Blade (perpendicular to Jet stream)

The starting fluid flow is V_1 and the water flow velocity precisely hit the blade is V_2 which is assumed to be 0 (zero). The distance between V_1 and V_2 is X, which is taken in t seconds (Fig. 3).

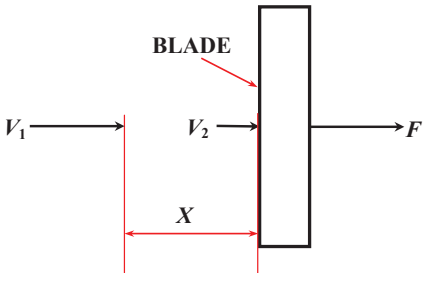

Fig. 3. Flat Blade momentum

The force acting on the blade can be calculated as follows.

$$F = \rho\cdot A\cdot\frac{X}{t}\left(V_1 - V_2\right),$$

$$F = \rho\cdot A\cdot V\left(V - 0\right),$$

$$F = \rho\cdot AV^2,$$

where ρ – density, kg/m^3; A – Jet cross-sectional area, m^2; V_1 – incoming Fluid Velocity, m/s; V_2 – out Fluid Velocity, m/s; F – Force acting on the blade, N.

4. 4. Angled Blade (Against the Jet stream)

Assume that V is the fluid flow velocity. The perpendicular water flow velocity of the blade is $V_1 = V\cos\theta$. While V_2 = the fluid velocity precisely hits the blade, which is assumed to be 0 (zero). The distance between V_1 and V_2 is X, which is taken in t seconds (Fig. 4).

From the information F can be calculated as follows.

$$F = \rho\cdot A\cdot\frac{X}{t}\left(V_1 - V_2\right),$$

$$F = \rho\cdot A\cdot V^2\left(V\cos\theta\right),$$

$$F = \rho\cdot A\cdot V^2\cdot\cos\theta,$$

where ρ – density, kg/m^3; A – Jet cross-sectional area, m^2; V_1 – incoming Fluid Velocity [m/s]; V_2 – End Fluid Velocity [m/s]; F – Force acting on the blade, N.

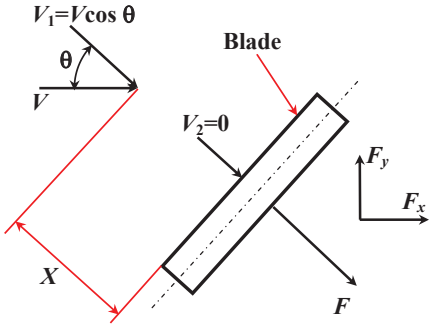

Fig. 4. Angled blade momentum

4. 5. Curved Blade

The turbo engine utilizes force due to fluid through a moving blade. There is no work that can be done against or by the fluid flowing through the fixed blade. If the blade can move, then work can be done on the blade or fluid. Forces carried out by the blade are indicated by F_x and F_y. Then the control volume contains fluid in sections 1 and 2. Absolute velocity vectors start at zero, and the relative velocity vector V_0–u rotates through the angle θ as shown Fig. 5. V_2 is the absolute final speed that leaves the blade. Relative speed v_r=V_0–u does not change the size along the trip through the blade. The period per unit time is given by ρA_0v_r.

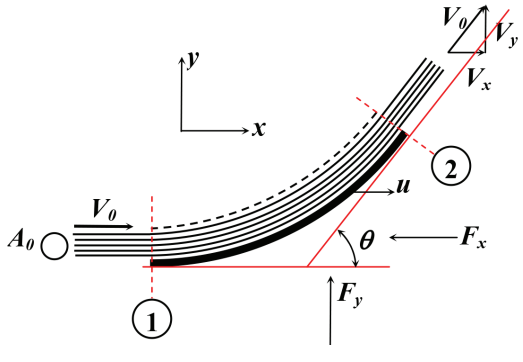

Fig. 5. Curved Blade Momentum

The application of the equation in the volume control (Fig. 5) gives the force equation as follows.

$$F_x = \rho \cdot (V_0 - u)^2 \cdot A_0 \cdot (1 - \cos\theta),$$

$$F_y = \rho \cdot (V_0 - u)^2 \cdot A_0 \sin\theta,$$

where ρ – density, kg/m^3; A – Jet cross-sectional area, m^2; V_0 – incoming Fluid Velocity, m/s; F_x – Force acting on the blade on the x-axis direction, N; F_y – Force acting on the blade on the y-axis direction, N; u – the blade velocity movement, m/s.

Therefore, through this investigation, it is expected that the turbine performance will increase. Investigation of turbine performance in this study is to conduct a simulation investigation using Computer Fluid Dynamic (CFD) technology. The type of kinetic turbine that will be investigated is the bowl bladed kinetic turbine. Bowl bladed kinetic turbine was chosen in this study because the curved blade kinetic turbine has been studied and the results are quite satisfactory [20]. Another reason why this investigation is carried out with simulation is, firstly, by a simulation research, the research will be low in cost, because modifications to the model can be done anytime. The modification can be very easily be done by utilizing the existing facilities in the CFD software. Secondly, if the research is carried out by experiments in the laboratory, the modification process will be more complicated and the costs required will also be high. The purpose of this research is to simulate the bowl bladed kinetic turbine performance. So the simulation research in this study is to compare the conventional bowl bladed kinetic turbine (Fig. 6) with a bowl bladed kinetic turbine that was given an additional steering blade (Fig. 7). Based on the consideration of the momentum that occurs in the blade, the addition of the steering blade is expected to increase the overall kinetic momentum of this turbine. The additional steering blade investigation has been carried out in previous studies conducted on the curve blade kinetic turbine [21].

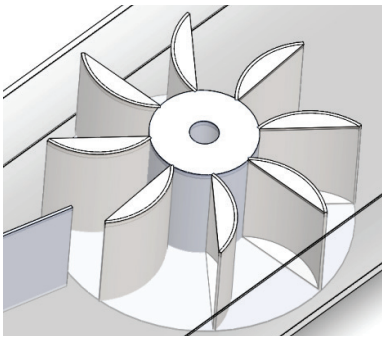

Fig. 6. Bowl Bladed Kinetic Turbine

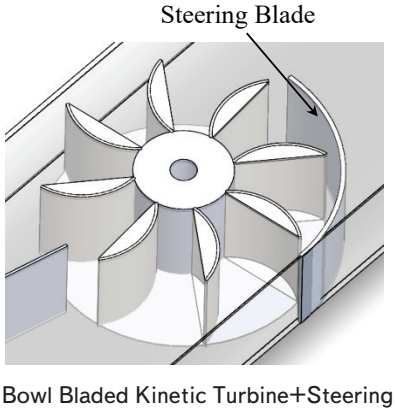

Fig. 7. Bowl Bladed Kinetic Turbine+Steering Blade

5. Material and methods

5. 1. Bowl bladed kinetic turbine

A kinetic turbine is a simple turbine that just depends on the fluid flow energy. Kinetic turbine is the development of a water wheel that moves on the horizontal axis. To get better performance, the blade shape that was flat was designed to be a curved blade to get a greater momentum. Furthermore, the curve blade kinetic turbine was further developed, so that performance improved again, by turning the blade into a bowl shape. The selection of the kinetic turbine blade into the bowl shape is adopting the pelton turbine blade shape.

The purpose of forming this bowl shaped blade is that the momentum generated will be greater. The bowl bladed kinetic turbine shape is shown in Fig. 8.

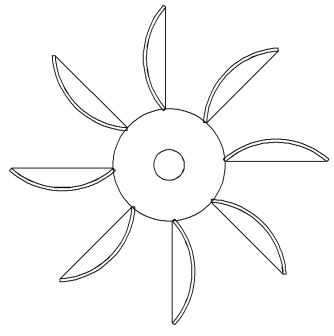

Fig. 8. Bowl bladed kinetic turbine

This bowl bladed kinetic turbine (BBKT) was already investigated by several researchers, both tested experimentally and tested with computational fluid dynamic (CFD). Whereas this research is the development of the BBKT by adding a steering blade and testing using CFD.

5. 2. Computational Fluid Dynamics

Quantitatively the flow type can be known based on the ratio between the inertial force (vsρ) toward the viscous force (μ/L) which is defined as the Reynold number.

$$Re = \frac{VD_p}{\mu}, \quad (1)$$

where V – fluid speed, m/s; D – pipe diameter, m; ρ – fluid density, kg/m^3; μ – fluid dynamic viscosity, kg/m·s or N·s/m^2.

Computational fluid dynamics is the study of fluid flow patterns which also include fluid flow rates, pressure, mass, discharge and other phenomena. In predicting a flow pattern, several equations are used to set the mathematical model to find the value of the parameters observed in the flow. And the main purpose of the CFD is to provide a deeper understanding of experimental research.

In general, the fluid flow applies the energy equation, momentum and continuity equation.

a. Continuity Equation

$$\frac{\partial \rho}{\partial t} + \frac{\partial(\rho u)}{\partial x} + \frac{\partial(\rho v)}{\partial y} = 0. \quad (2)$$

b. Momentum

Momentum on x axis:

$$\frac{\partial(\rho u)}{\partial t} + \frac{\partial(\rho u^2)}{\partial x} + \frac{\partial(\rho uv)}{\partial y} = -\frac{\partial p}{\partial y} + \frac{1}{Re_r}\left(\frac{\partial t_{xx}}{\partial x} + \frac{\partial t_{xy}}{\partial y}\right). \quad (3)$$

Momentum on y axis:

$$\frac{\partial(\rho v)}{\partial t} + \frac{\partial(\rho uv)}{\partial x} + \frac{\partial(\rho v^2)}{\partial y} = -\frac{\partial p}{\partial y} + \frac{1}{Re_r}\left(\frac{\partial t_{xy}}{\partial x} + \frac{\partial t_{yy}}{\partial y}\right), \quad (4)$$

where ρ – fluid density, kg/m^3; t – time, s; u, v – fluid velocity on x- and y-axis, m/s; P – pressure, N/m^2; Re – Reynolds number.

Basically computational fluid dynamics replaces partial differential equations of continuity, momentum and energy with an algebraic equation. The equation whose origin is continuum (has an infinite number of cells) is converted into a discrete model (finite cell number).

In general, the stages of work are divided into 3 steps, namely: Pre-processing, Processing, Post processing.

5. 3. Experimental study

Two-dimensional numerical simulations with transient state conditions are carried out using software based on the finite element method. Transient conditions are based on the fact that in all actual conditions, all physical phenomena need time to reach a steady or stable state. The transition from an unstable condition to achieving a stable condition at a certain time interval is called a transient state.

The first step is to create a turbine kinetic geometry with dimensions, as shown in Fig. 9.

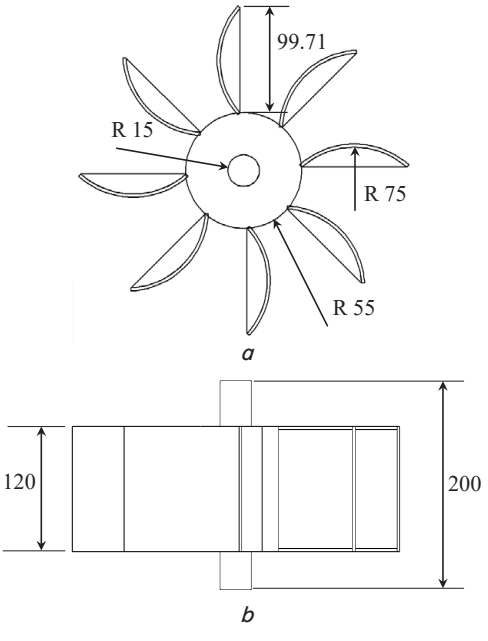

Fig. 9. Bowl bladed kinetic turbine dimension: *a* – Top view; *b* – Side View

The second step is to make the duct geometry as shown in Fig. 10. The geometry of a kinetic turbine installation includes: a water flow channel with a length of 1,500 mm, a height of 120 mm, a duct width of 350 mm, a guide blade angle of 14.5° and a steering blade with a radius of 175 mm.

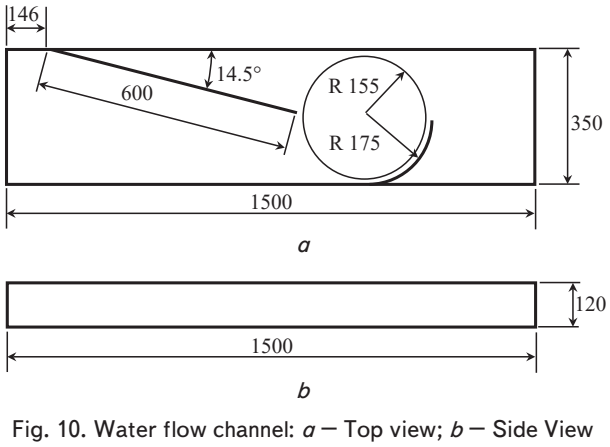

Fig. 10. Water flow channel: *a* – Top view; *b* – Side View

This water flow channel is a duct for the water flow which will be simulated as kinetic energy to drive the hydrokinetic turbine.

The next step is to assemble the complete unit by inserting the turbine into the water flow channel (duct). As shown in Fig. 11.

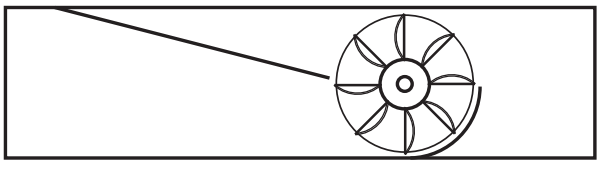

Fig. 11. Complete installation (Top View)

The next step is the meshing process. Where the meshing system used is the automatic meshing system. Choosing the automatic meshing system is believed to be able to produce the desired results. This mesh system would choose the best total cell amount. In this case, the total fluid cells are 25,700 cells (Fig. 12).

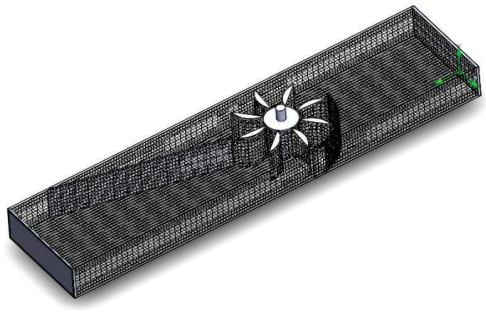

Fig. 12. Meshing

The next step is setting the Boundary Condition. The boundary conditions are the inlet water flow parameters and outlet parameters. For the inlet parameters, some condition could be chosen, such as the; inlet mass flow, the inlet volume flow or the inlet water velocity. For the inlet parameters, firstly, choose the inlet face duct flow, next is choosing the inlet water flow parameter, in this case the inlet volume flow was chosen with a water flow rate of 0.05 m^3/s. For the outlet parameter the environmental pressure with a pressure of 101,325 Pa was chosen and a temperature of 298.2 K (Fig. 13).

Lastly, run the active project to execute the simulation process. After the running execution finished, then determine the pressure surface plot.

6. Results of the CFD simulation

From the CFD simulation result, pressure contours on the object result based on the turbine runner angle position could be seen. The runner angle position is divided in every 5° rotation movement, starts from 5° until 45°. Every result is a pair of figure that represents a bowl bladed kinetic turbine with and without a steering blade.

Pressure contours that occur in the CFD simulation on a BBKT without a steering blade at a 5° turbine rotor position (Fig. 14).

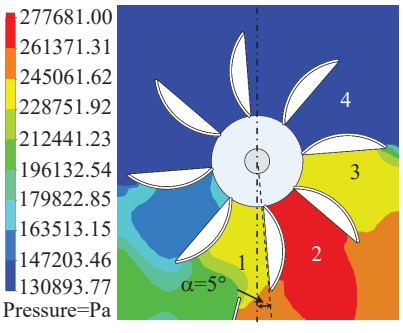

Fig. 14. Pressure contour α=5°, BBKT without a steering blade

Pressure contours that occur in the CFD simulation on a BBKT with a steering blade at a 5° turbine rotor position (Fig. 15).

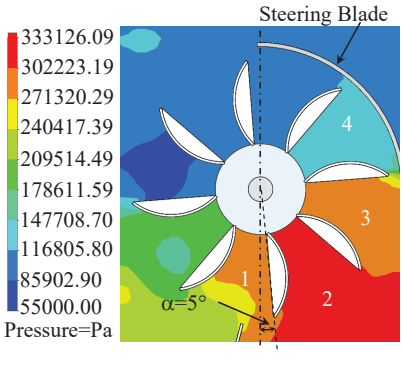

Fig. 15. Pressure contour α=5°, BBKT with a steering blade

Pressure contours that occur in the CFD simulation on a BBKT without a steering blade at a 10° turbine rotor position (Fig. 16).

Pressure contours that occur in the CFD simulation on a BBKT with a steering blade at a 10° turbine rotor position (Fig. 17).

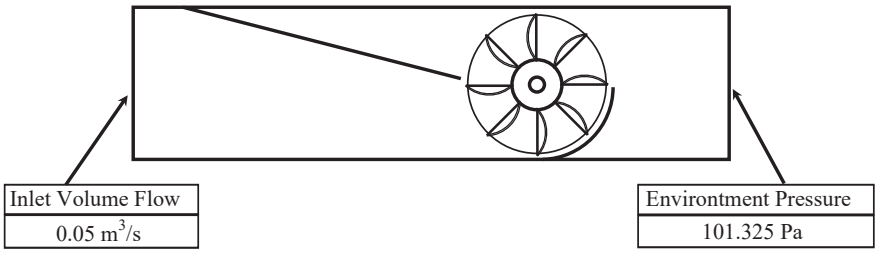

Fig. 13. Hydrokinetic Turbine Boundary conditions

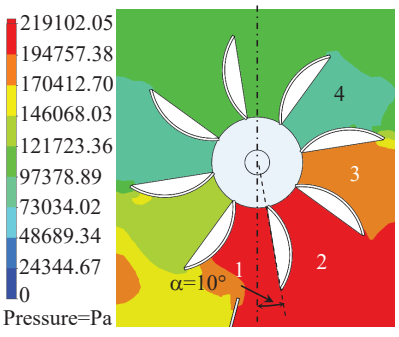

Fig. 16. Pressure contour α=10°, BBKT without a steering blade

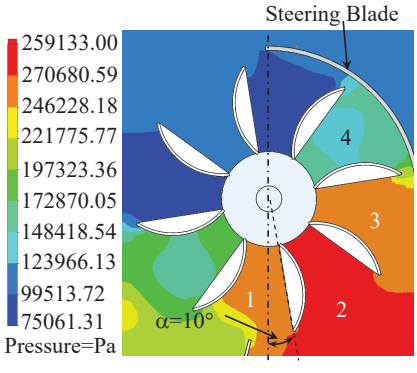

Fig. 17. Pressure contour α=10°, BBKT with a steering blade

Pressure contours that occur in the CFD simulation on a BBKT without a steering blade at a 15° turbine rotor position (Fig. 18).

Pressure contours that occur in the CFD simulation on a BBKT with a steering blade at a 15° turbine rotor position (Fig. 19).

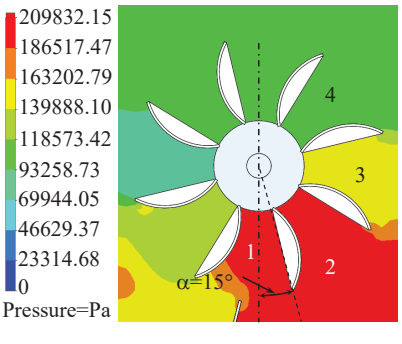

Fig. 18. Pressure contour α=15°, BBKT without a steering blade

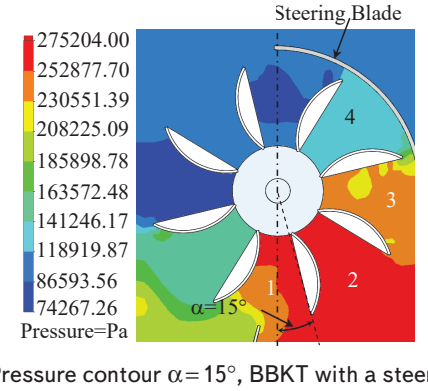

Fig. 19. Pressure contour α=15°, BBKT with a steering blade

Pressure contours that occur in the CFD simulation on a BBKT without a steering blade at a 20° turbine rotor position (Fig. 20).

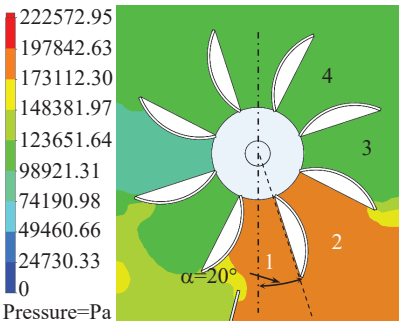

Fig. 20. Pressure contour α=20°, BBKT without a steering blade

Pressure contours that occur in the CFD simulation on a BBKT with a steering blade at a 20° turbine rotor position (Fig. 21).

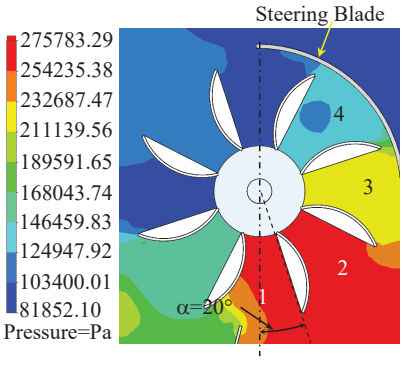

Fig. 21. Pressure contour α=20°, BBKT with a steering blade

Pressure contours that occur in the CFD simulation on a BBKT without a steering blade at a 25° turbine rotor position (Fig. 22).

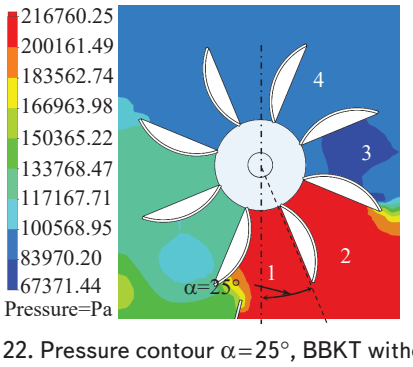

Fig. 22. Pressure contour α=25°, BBKT without a steering blade

Pressure contours that occur in the CFD simulation on a BBKT with a steering blade at a 25° turbine rotor position (Fig. 23).

Pressure contours that occur in the CFD simulation on a BBKT without a steering blade at a 30° turbine rotor position (Fig. 24).

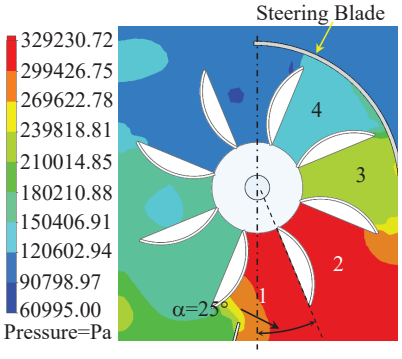

Fig. 23. Pressure contour α=25°, BBKT with a steering blade

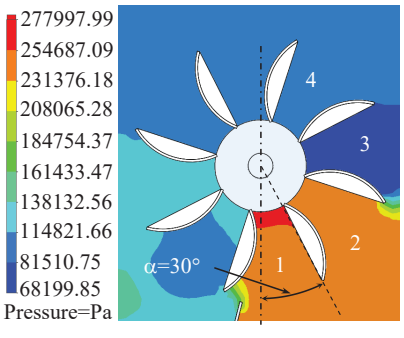

Fig. 24. Pressure contour α=30°, BBKT without a steering blade

Pressure contours that occur in the CFD simulation on a BBKT with a steering blade at a 30° turbine rotor position (Fig. 25).

Pressure contours that occur in the CFD simulation on a BBKT without a steering blade at a 35° turbine rotor position (Fig. 26).

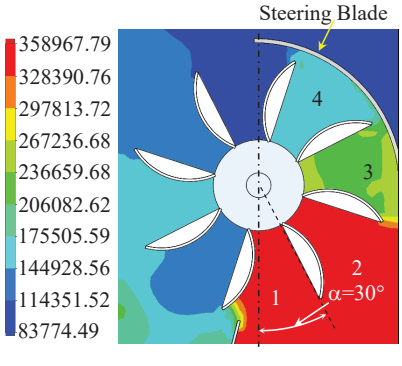

Fig. 25. Pressure contour α=30°, BBKT with a steering blade

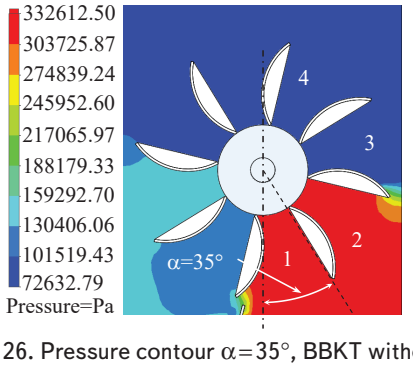

Fig. 26. Pressure contour α=35°, BBKT without a steering blade

Pressure contours that occur in the CFD simulation on a BBKT with a steering blade at a 35° turbine rotor position (Fig. 27).

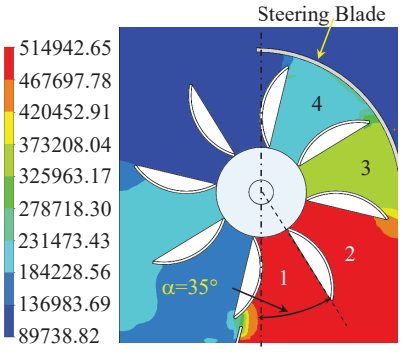

Fig. 27. Pressure contour α=35°, BBKT with a steering blade

Pressure contours that occur in the CFD simulation on a BBKT without a steering blade at a 40° turbine rotor position (Fig. 28).

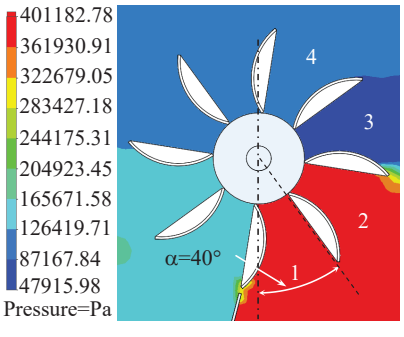

Fig. 28. Pressure contour α=40°, BBKT without a steering blade

Pressure contours that occur in the CFD simulation on a BBKT with a steering blade at a 40° turbine rotor position (Fig. 29).

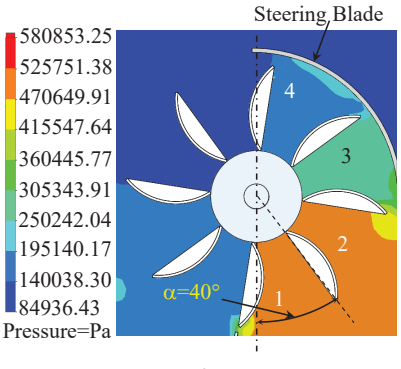

Fig. 29. Pressure contour α=40°, BBKT with a steering blade

Pressure contours that occur in the CFD simulation on a BBKT without a steering blade at a 45° turbine rotor position (Fig. 30).

Pressure contours that occur in the CFD simulation on a BBKT with a steering blade at a 45° turbine rotor position (Fig. 31).

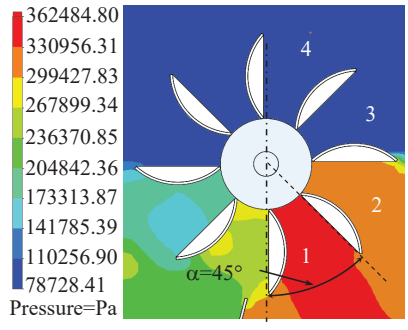

Fig. 30. Pressure contour α=45°, BBKT without a steering blade

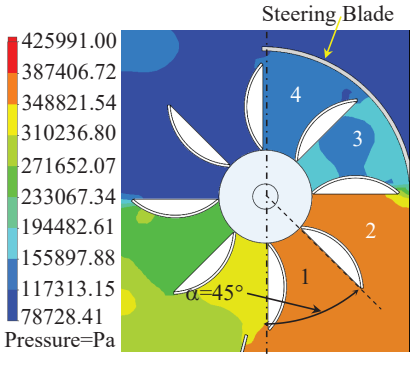

Fig. 31. Pressure contour α=45°, BBKT with a steering blade

From the simulation results, the pressure that occurs in area 1 can be taken. The pressure in area 1 on every runner position is then taken either in the bowl bladed kinetic turbine without a steering blade or the bowl bladed kinetic turbine with a steering blade. The water pressure reading results can be seen in Table 1.

Table 1

Pressure in area 1 for each runner position angle

α, °	P_1, Pa	P_2, Pa
5	237,648	282557.7
10	199,183	275126.5
15	190756.5	258163.6
20	182,105	258153.2
25	209979.9	304845.7
30	249389.2	340875.4
35	332612.5	568942.7
40	401182.8	691377.1
45	420,039	503,161

With a is the runner position angle; P_1 is the pressure between two blades on the BBKT without a steering blade; P_2 is the pressure between two blades on the BBKT with a steering blade.

From the data in Table 1, the BBKT pressure in area 1 is expressed in graphical form to make it easier to see the results as shown in Fig. 32.

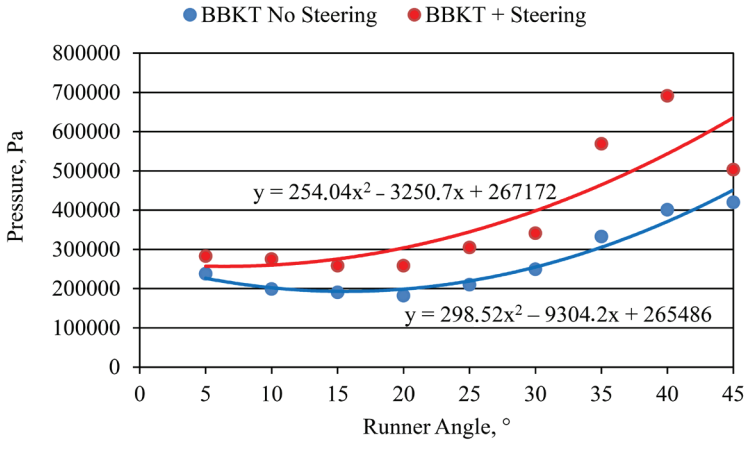

Fig. 32. Graph of pressure comparison in area 1 between bowl bladed kinetic turbine without steering blade and bowl bladed kinetic turbine with steering blade for each turbine runner angle position

From the simulation results, the pressure that occurs in area 1–4 can be taken. The pressure in area 1–4 on every runner position is then taken either in the bowl bladed kinetic turbine (BBKT) without a steering blade or the bowl bladed kinetic turbine with a steering blade. The water pressure reading results can be seen in Table 2.

Table 2

Total pressure area 1–4 for each runner position angle

α, °	P_1, Pa	P_2, Pa
10	727,754	980,465
15	648,571	945,415
20	622,310	891,570
25	622,615	1,024,300
30	662,025	1,045,420
35	881,392	1,582,617
40	962,426	2,103,936
45	954,633	1,433,871

With a is the runner position angle; P_1 is the pressure between two blades on the BBKT without a steering blade; P_2 is the pressure between two blades on the BBKT with a steering blade. From the data in Table 2, the BBKT pressure in areas 1 to area 4 is expressed in graphical form to make it easier to see the results as shown in Fig. 33.

From the water flow trajectory, it was also seen that the water flow is not leaving the turbine area. The water flow was directed by the steering blade and giving an added push on the rest blades as seen in Fig. 34.

From the picture in Fig. 34, one of the CFD simulation, it can be seen that water flow after pushing the first blade, does not directly leave the turbine straight to the turbine discharge area. It appears that the water flow provides an additional impetus to the next blades. This phenomenon is expected to increase each turbine blade momentum. This momentum addition means there is an additional turbine torque. This additional turbine torque clearly results in a turbine performance increase.

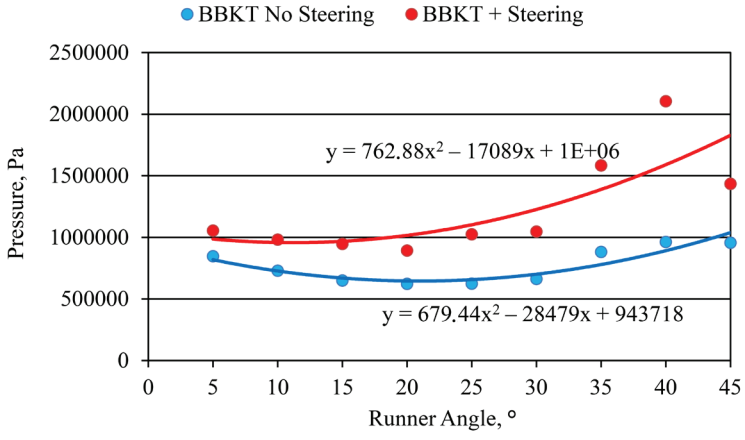

Fig. 33. Graph of total pressure comparison in area 1 to 4 between BBKT without steering blade and BBKT with steering blade for each turbine runner angle position

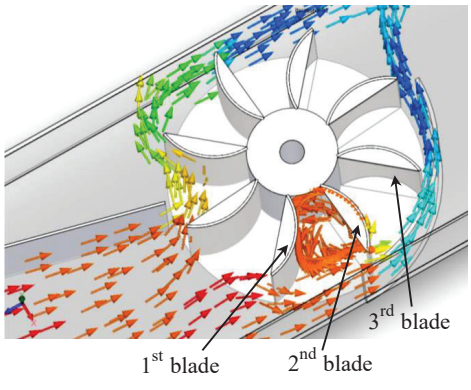

Fig. 34. Water flow pushing some more blades

7. Discussion of experimental results

The discussion in this section is comparing the water pressure between blades in the bowl bladed kinetic turbine without a steering blade and the bowl bladed kinetic turbine with a steering blade.

7. 1. Pressure comparison between a turbine with and without a steering blade on α=0° runner position

Fig. 14 shows the water pressure distribution between the turbine blades at α=0° runner position in a bowl bladed kinetic turbine without a steering blade. While Fig. 15 shows the water pressure distribution between blades, in a bowl bladed kinetic turbine with a steering blade.

There is a pressure increase in the turbine with the steering blade attached. This increase in pressure indicates that there is an increase in momentum which results in a turbine torque increase. The pressure between blades 2 and 3 in the turbine with the steering blade is 1.25e+010 Pa, while the water pressure is 9.81e+009 Pa on the turbine without the steering blade. So for the same blade position, there is a pressure increase in the turbine with the steering blade. While the lowest pressure that occurs between two blades is between blades 5 and 6. On the turbine with the steering blade, the pressure between the blade 5 and 6 is 4.46e+009 Pa, while the pressure on the turbine without the steering blade in the same position is 2.07e+009 Pa. So, the water pressure between two blades in the turbine with a steering blade has a higher value compared to the turbine without a steering blade. It should be added that the pressure between blade 3 and blade 4 also rises. In overall the pressure between the two blades increases.

7. 2. Pressure comparison between a turbine with and without a steering blade on α=5° runner position

Fig. 16 shows the water pressure distribution between the turbine blades at α=5° runner position in a bowl bladed kinetic turbine without a steering blade. While Fig. 17 shows the water pressure distribution between blades in a bowl bladed kinetic turbine with a steering blade.

For α=5° runner position, it can be seen that the pressure between the two blades on the turbine with a steering blade (Fig. 17) is higher compared to the pressure on the turbine without a steering blade (Fig. 16).

The pressure between blade 2 and blade 3 on the turbine with a steering blade is 9.60e+009 Pa, while in the turbine without a steering blade, the water pressure is 7.98e+009 Pa. So for the same blade position, there is an increase in water pressure between the blades in the turbine with the steering blade. While the lowest pressure that occurs between two blades is between blades 5 and 6. In the turbine with the steering blade, the pressure between blades 5 and 6 is 3.50e+008 Pa, while the pressure on the turbine without a steering blade in the same position is 10.00e+007 Pa. As in the runner position α=0°, the water pressure between the two blades in the turbine with the steering blade has a higher water pressure value compared to the turbine without the steering blade.

7. 3. Pressure comparison between a turbine with and without a steering blade on α=15° runner position

Fig. 18 shows the water pressure distribution between the turbine blades at α=5° runner position in a bowl bladed kinetic turbine without a steering blade. While Fig. 19 shows the water pressure distribution between blades, in a bowl bladed kinetic turbine with a steering blade.

For the runner position with α=15°, there is also an increase in water pressure between the two blades as shown in Fig. 16 and Fig. 17. This increase in pressure indicates that there is an increase in momentum resulting in an increase in turbine torque. The pressure between blade 2 and blade 3 in the turbine with a steering blade is 7.20e+009 Pa, while in the turbine without a steering blade, the water pressure is 4.74e+009 Pa. So for the same blade position, there is a pressure increase in the turbine with the steering blade. The increase in pressure also occurs between blades 3 and 4 with a maximum pressure and also an increase between blades 4 and 5. While the lowest pressure that occurs between two blades is between blades 5 and 6. In the turbine with a steering blade, the pressure between blades 5 and 6 is 1.94e+008 Pa, while the pressure on the turbine without a steering blade in the same position is 10.00e+007 Pa. So the water pressure between the two blades in the turbine with the steering blade has a higher value compared to the turbine without a steering blade.

7. 4. Pressure comparison between a turbine with and without a steering blade on α=20° runner position

Fig. 20 shows the water pressure distribution between the turbine blades at a runner position α=20° for the turbine

without a steering blade. Whereas the picture in Fig. 21 is a water pressure distribution between the blades at a runner position $\alpha=20°$ for the turbine with the steering blade.

For a runner position with $\alpha=20°$, there is also an increase in water pressure between two blades as shown in Fig. 20, 21. This increase in pressure indicates that there is an increase in momentum resulting in an increase in turbine torque. The pressure between blades 2 and 3 on the turbine with a steering blade is above 4.92e+009 Pa, whereas in the turbine without a steering blade the value of the water pressure is 3.89e+009 Pa. So for the same blade position, there is a pressure increase in the turbine with a steering blade. The increase in pressure also occurs between blades 3 and 4 and also between blades 4 and 5 with a maximum pressure. While the lowest pressure that occurs between the two blades is between blades 5 and 6. In the turbine with a steering blade, the pressure between blades 5 and 6 is 1.33e+008 Pa, while the pressure on the turbine without a steering blade in the same position is 10.00e+007 Pa. So the water pressure between the two blades in the turbine with the steering blade has a higher value compared to the turbine without the steering blade.

7. 5. Pressure comparison between a turbine with and without a steering blade on $\alpha=25°$ runner position

Fig. 22 shows the water pressure distribution between the turbine blades at a runner position $\alpha=25°$ for the turbine without the steering blade. Whereas the picture in Fig. 23 is a water pressure distribution between the blades at a runner position $\alpha=25°$ for the turbine with a steering blade.

For the runner position with $\alpha=25°$, there is also an increase in water pressure between the two blades as shown in Fig. 22 and Fig. 23. This increase in pressure indicates that there is an increase in momentum which results in an increase in turbine torque. The pressure between blades 2 and 3 in the turbine with the steering blade is above 4.92e+009 Pa, while in the turbine without the steering blade the value of the water pressure is 4.28e+009 Pa. So for the same blade position, there is a pressure increase in the turbine with the steering blade. The increase in pressure also occurs between blades 3 and 4 and also between blades 4 and 5 with a maximum pressure. While the lowest pressure that occurs between two blades is between blades 5 and 6. In the turbine with the steering blade, the pressure between blades 5 and 6 is 1.83e+008 Pa, while the pressure on the turbine without the steering blade in the same position is 10.00e+007 Pa. So the water pressure between the two blades in the turbine with the steering blade has a higher value compared to the turbine without the steering blade.

7. 6. Pressure comparison between a turbine with and without a steering blade on $\alpha=30°$ runner position

Fig. 24 shows the water pressure distribution between the turbine blades at the runner position $\alpha=30°$ for the turbine without the steering blade. Whereas the picture in Fig. 25 is a water pressure distribution between the blades at the runner position $\alpha=30°$ for the bowl bladed kinetic turbine with the steering blade.

For the runner position with $\alpha=30°$, there is also an increase in water pressure between the two blades as shown in Fig. 24, 25. This increase in pressure indicates that there is an increase in momentum which results in an increase in turbine torque. The pressure between blades 2 and 3 in the turbine with the steering blade is above 7.89e+009 Pa, while in the turbine without the steering blade the water pressure value is 6.23e+009 Pa. So for the same blade position, there is a pressure increase in the turbine with the steering blade. The increase in pressure also occurs between blades 3 and 4 and also between blades 4 and 5 with a maximum pressure. While the lowest pressure that occurs between two blades is between blades 5 and 6. In the turbine with the steering blade, the pressure between blades 5 and 6 is 1.20e+008 Pa, while the pressure on the turbine without the steering blade in the same position is 10.00e+007 Pa. So the water pressure between the two blades in the turbine with the steering blade has a higher value compared to the turbine without the steering blade.

7. 7. Pressure comparison between a turbine with and without a steering blade on $\alpha=35°$ runner position

Fig. 26 shows the water pressure distribution between the turbine blades at the runner position $\alpha=35°$ for the turbine without a steering blade. Whereas the picture in Fig. 27 is a water pressure distribution between the blades at the runner position $\alpha=35°$ for the bowl bladed kinetic turbine with a steering blade.

For the runner position with $\alpha=35°$, there is also an increase in water pressure between the two blades as shown in Fig. 26, 27. This increase in pressure indicates that there is an increase in momentum which results in an increase in turbine torque. The pressure between blades 2 and 3 in the turbine with the steering blade is above 9.00e+009 Pa, while in the turbine without the steering blade the value of the water pressure is 6.94e+009 Pa. So for the same blade position, there is a pressure increase in the turbine with the steering blade. The increase in pressure also occurs between blades 3 and 4 with maximum pressure and also a rise in pressure between blades 4 and 5. While the lowest pressure that occurs between the two blades is between blades 5 and 6. In the turbine with the steering blade, the pressure between blades 5 and 6 is 1.58+008 Pa, while the pressure on the turbine without the steering blade in the same position is 10.00e+007 Pa. So the water pressure between the two blades in the turbine with the steering blade has a higher value compared to the turbine without the steering blade.

7. 8. Pressure comparison between a turbine with and without a steering blade on $\alpha=40°$ runner position

Fig. 28 shows the water pressure distribution between the turbine blades at the runner position $\alpha=40°$ for the turbine without the steering blade. Whereas the picture in Fig. 29 is a water pressure distribution between the blades at the runner position $\alpha=40°$ for the bowl bladed kinetic turbine with the steering blade.

For the runner position with $\alpha=40°$, there is also an increase in water pressure between the two blades as shown in Fig. 28, 29. This increase in pressure indicates that there is an increase in momentum which results in an increase in turbine torque. The pressure between blades 2 and 3 in the turbine with the steering blade is above 9.00e+009 Pa, whereas in the turbine without the steering blade the water pressure value is 6.94e+009 Pa. So, for the same blade position, there is a pressure increase in the turbine with the steering blade. The increase in pressure also occurs between blades 3 and 4 with a maximum pressure and also a rise in pressure between blades 4 and 5. While the lowest pressure that occurs between the two blades is between blades 5 and 6. In the turbine with the steering blade, the pressure between blades 5 and 6 is 1.58+008 Pa, while the pressure on the turbine without the steering blade in the same position is 10.00e+007 Pa. So the water pressure between the two blades in the turbine with the steering blade has a higher value compared to the turbine without the steering blade.

7. 9. Pressure comparison between a turbine with and without a steering blade on α=45° runner position

Fig. 30 shows the water pressure distribution between the turbine blades at the runner position α=45° for the turbine without the steering blade. Whereas the picture in Fig. 31 is a water pressure distribution between the blades at the runner position α=45° for the bowl bladed kinetic turbine with the steering blade.

For the runner position with α=45°, there is also an increase in water pressure between the two blades as shown in Fig. 30, 31. This increase in pressure indicates that there is an increase in momentum which results in an increase in turbine torque. The pressure between blades 2 and 3 in the turbine with a steering blade is above 1.56e+010 Pa, while in the turbine without a steering blade, the water pressure is 1.23e+010 Pa. So for the same blade position, there is a pressure increase in the turbine with the steering blade. The increase in pressure also occurs between blades 3 and 4 with maximum pressure and also a rise in pressure between blades 4 and 5. While the lowest pressure that occurs between the two blades is between blades 5 and 6. In the turbine with a steering blade, the pressure between blades 5 and 6 is 9.63e+008 Pa, while the pressure on the turbine without the steering blade in the same position is 10.00e+007 Pa. So, the water pressure between the two blades in the turbine with the steering blade has a higher value compared to the turbine without the steering blade.

8. Conclusions

1. In general, there is an increase in the performance of the bowl bladed kinetic turbine added with a steering blade. As is known, the increase in pressure on the surface of the blade will increase the blade thrust per unit area. This increase in thrust (*F*) will increase momentum, which means there is an increase in turbine performance. Every water pressure (Pa) would result in a specific energy per volume (J/m^3).

2. It can be seen that the water pressure that occurs on the BBKT with a steering blade is always higher compared to the pressure occurred on the BBKT without a steering blade.

3. The overall thrust force in the turbine is the sum of the thrust force in each blade. By reviewing the total thrust on the four turbine blades, it can be seen that the overall thrust of the BBKT with a steering blade is always higher than the overall trust in the BBKT without a steering blade. This condition always occurred on every turbine runner angle position.

4. From the results of the pressure seen in the contour result from the simulation, there are at least three figures which get a pressure above 250,000 Pa.

References

1. Rispiningtati, Soenoko, R. (2015). Regulation of sutami reservoir to have a maximal electrical energy. International Journal of Applied Engineering Research, 10 (12), 31641–31648.
2. Indonesia Energy Outlook (2016). Agency for the Assessment and Application of Technology.
3. Yang, B., Lawn, C. (2011). Fluid dynamic performance of a vertical axis turbine for tidal currents. Renewable Energy, 36 (12), 3355–3366. doi: https://doi.org/10.1016/j.renene.2011.05.014
4. Yang, B., Lawn, C. (2013). Three-dimensional effects on the performance of a vertical axis tidal turbine. Ocean Engineering, 58, 1–10. doi: https://doi.org/10.1016/j.oceaneng.2012.09.020
5. Golecha, K., Eldho, T. I., Prabhu, S. V. (2011). Investigation on the Performance of a Modified Savonius Water Turbine with Single and Two deflector Plates. The 11th Asian International Conference on Fluid Machinery and Fluid Power Technology.
6. Sinagra, M., Sammartano, V., Aricò, C., Collura, A., Tucciarelli, T. (2014). Cross-flow Turbine Design for Variable Operating Conditions. Procedia Engineering, 70, 1539–1548. doi: https://doi.org/10.1016/j.proeng.2014.02.170
7. Sammartano, V., Aricò, C., Sinagra, M., Tucciarelli, T. (2015). Cross-Flow Turbine Design for Energy Production and Discharge Regulation. Journal of Hydraulic Engineering, 141 (3), 04014083. doi: https://doi.org/10.1061/(asce)hy.1943-7900.0000977
8. Lopes, J. J. A., Vaz, J. R. P., Mesquita, A. L. A., Mesquita, A. L. A., Blanco, C. J. C. (2015). An Approach for the Dynamic Behavior of Hydrokinetic Turbines. Energy Procedia, 75, 271–276. doi: https://doi.org/10.1016/j.egypro.2015.07.334
9. Tian, W., Mao, Z., Ding, H. (2018). Design, test and numerical simulation of a low-speed horizontal axis hydrokinetic turbine. International Journal of Naval Architecture and Ocean Engineering, 10 (6), 782–793. doi: https://doi.org/10.1016/j.ijnaoe.2017.10.006
10. Sukmawaty, S., Firdaus, N., Putra, G. M. D., Ajeng, S. D. (2018). Effect of Blade number and Directional Plate Angle on Kinetic Turbine Performances. International Journal of Mechanical Engineering and Technology (IJMET), 9 (13), 395–402.
11. Jaini, Kaprawi, Santoso, D. (2015). Darrieus Water Turbine Performance Configuration of Blade. Journal of Mechanical Science and Engineering, 2 (1), 7–11.
12. Hantoro, R., Septyaningrum, E. (2018). Novel Design of a Vertical Axis Hydrokinetic Turbine – Straight-Blade Cascaded (VAHT–SBC): Experimental and Numerical Simulation. Journal of Engineering and Technological Sciences, 50 (1), 73–86. doi: https://doi.org/10.5614/j.eng.technol.sci.2018.50.1.5
13. Zanforlin, S., Burchi, F., Bitossi, N. (2016). Hydrodynamic Interactions Between Three Closely-spaced Vertical Axis Tidal Turbines. Energy Procedia, 101, 520–527. doi: https://doi.org/10.1016/j.egypro.2016.11.066
14. Góralczyk, A., Adamkowski, A. (2018). Model of a Ducted Axial-Flow Hydrokinetic Turbine – Results of Experimental and Numerical Examination. Polish Maritime Research, 25 (3), 113–122. doi: https://doi.org/10.2478/pomr-2018-0102
15. Anyi, M., Kirke, B. (2010). Evaluation of small axial flow hydrokinetic turbines for remote communities. Energy for Sustainable Development, 14 (2), 110–116. doi: https://doi.org/10.1016/j.esd.2010.02.003
16. Boedi, S. D., Soenoko, R., Wahyudi, S., Choiron, M. A. (2015). An Outer Movable Blade Vertical Shaft Kinetic Turbine Performance. International Journal of Applied Engineering Research, 10 (4), 8565–8573.

17. Soenoko, R., Setyarini, P. H., Gapsari, F. (2018). Bowl Bladed Hydro Kinetic Turbine Performance. ARPN Journal of Engineering and Applied Sciences, 13 (20), 8242–8250.
18. Kumar, A., Nikhade, A. (2014). Hybrid Kinetic Turbine Rotors: A Review, International Journal of Engineering Science & Advanced Technology, 4 (6), 453–463.
19. Streeter, V. L., Wylie E. B., Bedford, K. W. (1997). Fluid Mechanics. McGraw-Hill College.
20. Soenoko, R., Setyarini, P. H., Gapsari, F. (2018). Numerical modeling and investigation of hydrokinetic turbine with additional steering blade using CFD. ARPN Journal of Engineering and Applied Sciences, 13 (22), 8589–8598.

Проаналізовано особливості функціонування електропривода запірної арматури. Встановлено, що привод запірної арматури, реалізований на базі асинхронних двигунів, характеризується низькою енергоефективністю. Для цілеспрямованого поліпшення енергетичних показників електроприводу розроблено метод оцінки енергетичної ефективності модуля арматури. Необхідність розробки метода викликана тим, що оцінки енергоефективності, засновані на міжнародних стандартах, справедливі для сталих режимів роботи, за умови нехтування часом перехідних процесів.

На відміну від традиційних типів приводів, привод запірної арматури характеризується низькими швидкостями обертання. Використання механічних редукторів не дозволяє істотно знизити швидкість приводу, тому доводиться здійснювати імпульсне керування двигуном або переходити на безредукторний привод.

Ефективність альтернативних типів двигунів оцінюється за допомогою запропонованого метода, який базується на моделюванні процесу позиціонування запірної арматури. Траєкторія переміщення формується відповідно до керуючих імпульсів, які подаються на обмотки двигуна, що входить до складу мехатронного модуля.

Апробація методу проведена відповідно до паспортних даних асинхронного двигуна типу AIP56A4, потужністю 120 Вт, що входить до складу однооборотного мехатронного модуля, та випускається серійно. Для порівняння енергетичних показників обрано 3-х фазний синхронний двигун з ротором, що котиться, у якого параметри обмотки статора аналогічні параметрам обмотки двигуна AIP56A.

Порівняння оцінок енергетичної ефективності показало перевагу і перспективність використання безредукторних синхронних двигунів в приводі запірної арматури.

Розроблені моделі дозволяють досліджувати і оптимізувати характеристики електроприводу на базі двигунів, що досліджуються, а також формулювати вимоги до конструктивно-технологічних параметрів двигуна на основі одержуваних оцінок енергоефективності.

Запропонована методика оцінки енергоефективності є основою для реалізації комплексу технічних засобів, що забезпечують оцінку енергоефективності приводу в реальних промислових умовах, при виконанні конкретної технологічної задачі

Ключові слова: асинхронний двигун, безредукторний електропривод, енергоефективність модуля запірної арматури, синхронний реактивний двигун

UDC 62-83:621.313.392
DOI: 10.15587/1729-4061.2019.174203

ASSESSMENT OF EFFICIENCY OF ELECTRIC DRIVE OF STOP VALVES

H. Kulinchenko
PhD, Associate Professor*
E-mail: georgv@ukr.net
A. Masliennikov
PhD, Associate Professor
Department of Electrical Mashines
National Technical University
«Kharkiv Polytechnic Institute»
Kyrpychova str., 2,
Kharkiv, Ukraine, 61002
E-mail: x-maslennikov@yandex.ua
V. Bahuta
Technical Director
Ltd «Zodiak»
6 Hvardiyskoi dyviziyi str., 5,
Shostka, Ukraine, 44110
E-mail: viktrbaguta@gmail.com
V. Chervyakov
PhD, Associate Professor*
E-mail: vladymirchervyakov@gmail.com
*Department of Computer Science
Sumy State University
Rymskoho-Korsakova str., 2,
Sumy, Ukraine, 40007

Received date 19.04.2019
Accepted date 27.06.2019
Published date 19.08.2019

1. Introduction

The operational characteristics of stop valves (SV) depend on the type of actuator used. The requirements that are imposed on the SV drive in alternating load cycles are contradictory. A compromise between the minimum response time of the valves and the need to keep the load torque, which varies over a wide range, is usually achieved as a result of the search for the optimum.

The widespread use of pneumatic actuators for the SV in various industries was based on the idea of insufficient dynamics of the SV drive. Expansion of the nomenclature and required ranges of developed power of commercially available types of electric motors made it possible to solve